Fabrication of red blood cell-based multimodal theranostic probes for second near-infrared window fluorescence imaging-guided tumor surgery and photodynamic therapy

Peiyuan Wang[1,2,3], Xuandong Wang[1,2,3], Qiang Luo[1,2,3], Yang Li[1,2,3], Xiaoxiao Lin[1,2,3], Lingling Fan[4], Yun Zhang[1,2,3], Jingfeng Liu[1,2,3*], Xiaolong Liu[1,2,3*]

[1.] Key Laboratory of Design and Assembly of Functional Nanostructures, Fujian Institute of Research on the Structure of Matter, Chinese Academy of Sciences, Fuzhou 350002, P. R. China.

[2.] The United Innovation of Mengchao Hepatobiliary Technology Key Laboratory of Fujian Province, Mengchao Hepatobiliary Hospital of Fujian Medical University, Fuzhou 350025, P. R. China.

[3.] Department of Translational Medicine, Xiamen Institute of Rare Earth Materials, Chinese Academy of Sciences, Xiamen 361024, P. R. China.

[4.] Obstetrics and Gynecology Hospital, Fudan University, Shanghai 200011, P. R. China.

***Corresponding Authors:**

X. Liu. E-mail: xiaoloong.liu@gmail.com

J. Liu. E-mail: drjingfeng@126.com

Part A: Experimental Section

1. Materials and characterization

Materials. All solvents used were of analytical grade without further purification. Gadolinium (III) chloride anhydrous ($GdCl_3$, 99.99 %), erbium (III) chloride anhydrous ($ErCl_3$, 99.9 %), ytterbium (III) chloride anhydrous ($YbCl_3$, 99.9 %), thulium (III) chloride anhydrous ($TmCl_3$, 99.9 %), sodium trifluoroacetate (Na-TFA, 98 %), 1-octadecene (ODE, 90 %), oleic acid (OA, 90 %), Rose Bengal and hexanoic acid were supplied by Sigma Aldrich. Poly (ethylene glycol)–distearoyl phosphatidylethanolamine, ($DSPE\text{-}PEG_{2000}\text{-}NH_2$) and 1,2-distearoyl-sn-glycero-3-phosphoethanolamine-N-[biotinyl(polyethylene glycol)-2000] (ammonium salt) (DSPE-PEG2000-biotin) were purchased from Avanti Polar Lipids. RGD (Arg-Gly-Asp) peptides were purchased from Shanghai Qiangyao Biotechnology Co., Ltd.

Characterization. Transmission electron microscopy (TEM) measurements were carried out on a JEM 2100F microscope (Japan) operated at 200 kV. The samples were first dispersed in ethanol and then collected by using copper grids covered with carbon films for measurements. Scanning electron microscopic (SEM) images were obtained on a Philip XL30 microscope (Germany). A thin gold film was sprayed on the samples before characterization. UV–vis–NIR absorption spectra were measured on a Shimadz spectrophotometer (UV-3150) (Japan) with wavelength range of 300-1200 nm. NIR-II fluorescence spectra were recorded on Edinburgh Fluorescence Spectrometer FLS980 instrument with an external 808 nm semiconductor laser as excitation source (Changchun New Industries Optoelectronics Tech. Co., Ltd.), unless

otherwise specified, all spectra were collected under identical experimental conditions. NIR-II fluorescence imaging was carried by NIR vana InGaAs CCD camera under 808-nm irradiation. Visible Fluorescence spectra were recorded on Edinburgh Fluorescence Spectrometer FLS980 instrument with Xenon lamp as excitation source.

2. Synthesis of lanthanide doped core-shell structured $NaGdF_4$:Yb, Er@$NaGdF_4$ up-conversion nanoprobe.

Preparation of shell precursors for the synthesis of up-conversion nanoparticles

Gd-OA (0.10 M) host precursor: a mixture of $GdCl_3$ (2.50 mmol), OA (10.0 mL), and ODE (15.0 mL) was loaded in a reaction container and heated at 140 °C under vacuum with magnetic stirring for 30 min to remove residual water and oxygen. Then the colorless Gd-OA precursor solution (0.10 M) was obtained.

Yb-OA, Er-OA (0.1 M): The synthesis of Yb-OA and Er-OA precursor was carried out as the same as that of Gd-OA except 2.50 mmol of $YbCl_3$, 2.50 mmol of $ErCl_3$, were used instead of 2.5 mmol of $GdCl_3$, respectively.

Gd-Yb-Er-OA (0.10 M): Gd-Yb-Er-OA precursor was firstly obtained from a mixture of OA (10.0 mL), ODE (15.0 mL), Gd-OA (0.01 M), Yb-OA (0.01 M) and Er-OA (0.01 M) in a 78:20:2 ratio.

Na-TFA-OA (0.20 M) precursor: A mixture of Na-TFA (2.00 mmol) and OA (10.0 mL) was added into a container at room temperature under vacuum with magnetic stirring to remove residual water and oxygen. Then the colorless Na-TFA-OA

precursor solution (0.20 M) was obtained.

Synthesis of $NaGdF_4$:Yb,Er@$NaGdF_4$ UCNPs with a diameter of 40 nm: in a typical procedure for the synthesis of NaGdF4: 50 % Yb, 2 % Er nanocrystals, 0.48 mmol of anhydrous $GdCl_3$, 0.50 mmol of $YbCl_3$ and 0.02 mmol of $ErCl_3$ were added to a 100-mL flask containing 10 mL of oleic acid and 15 mL of 1-octadecene. The mixture was heated at 150 °C for 30 min before cooling down to 50 °C to remove the water content from the solution. Shortly thereafter, 10 mL of methanol solution containing NH_4F (2.75 mmol) and NaOH (2.5 mmol) was added and the resultant solution was stirred for 30 min to remove the methanol. After the methanol was evaporated, the solution was heated to 300 °C under argon for 1 h and then cooled down to room temperature. The resulting 35-nm $NaGdF_4$:Yb,Er nanoparticles were precipitated by addition of ethanol, collected by centrifugation at 6000 rpm for 5 min, washed with ethanol several times, and re-dispersed in 10 mL of cyclohexane. Then, 2.5 mL of the purified $NaGdF_4$:Yb,Er initial core solution was mixed with 4.0 mL of OA and 6.0 mL of ODE. The flask was pumped at 70 °C for 30 min to remove cyclohexane and residual air. Subsequently, the system was switched to air flow and the reaction mixture was further heated to 280 °C at a rate of ~ 20 °C/min. Then Gd-Yb-Er-OA (0.1 M, 1.0 mL) and Na-TFA-OA (0.20 M, 1 mL) host shell precursors were alternately introduced by dropwise addition at 280 °C and the time interval between each injection was 15 min. There are eight groups of Gd-Yb-Er-OA and Na-TFA-OA. Finally, the obtained $NaGdF_4$:Yb,Er@$NaGdF_4$ homogeneously doping cores were centrifuged and washed as above and dispersed in cyclohexane.

3. Oxygen and ICG release

Cell viability: HepG2 cells were cultured in DMEM low glucose medium containing 10 % fetal bovine serum (FBS) and 1 % penicillin/streptomycin at 37 °C under 5 % CO_2. Hypoxic Condition for HepG2 cell line was prepared under 93 % N_2 and 2 % O_2 in incubator. To carry out photodynamic therapy of cancer cells, HepG2 cells were collected through centrifugation and diluted to a density of $1* 10^4$ cells/mL in the DMEM low glucose medium and then seeded into 96-well plates (100 μL per well). After 24 h culturing, RBCp was added to the culture medium with five parallel wells for each concentration (0 ~ 250 μg/mL). Finally, after 24 h incubation, biocompatibility was evaluated by CCK-8 assay. For overcoming oxygen release, a power adjustable 808 nm fiber laser was collimated and employed as area light source to irradiate the HepG2 cells after cellular uptake of RBCp with 4 h in hypoxia condition. After 10 min exposure of 808 nm light at 0.5 W/cm^2, the cells were further incubated for additional 10 minutes and then irradiated by 980 nm light at 1.5 W/cm^2 for 15 minutes. Cell viability was measured by a CCK-8 kit. Cell viability of only RBCp, 980 nm laser, 808 nm laser, 808 nm + 980 nm and RBCp + 980 nm laser were also evaluated.

Dissolved O_2 detection: The △ dissolved O_2 was detected by dissolved oxygen meter. RBCp (100 μg/ml) was dispersed in PBS, then it was irradiated with 808 nm laser for different times. RBCp without 808 nm laser irradiation was carried out at the same time. Finally, the solution was collected and sealed for the dissolved O_2

concentration detection with dissolved oxygen meter.

Dissolved ICG detection: ICG release was also measured by UV-vis spectrometer as the same procedure of O_2 release.

***O_2 release in HepG2 cells*:** For O_2 release observation, $5*10^4$ cells were seeded in cell culture dish, after 24 h culturing in hypoxia condition, RBCp (150 μg/ml) was added into fresh medium and incubated for another 12 h. Then cells were treated with 808 nm NIR laser for various minutes (0 ~ 10 min), after incubation for another 30 min, cells were stained by tris(4,7-diphenyl-1,10-phenanthroline) ruthenium(II) dichloride ($Ru(dpp)_3^{2+}$) and DAPI for confocal laser scanning microscope (CLSM) observation of O_2 release in cytoplasm.

ROS detection in HepG2 cells: For ROS generation observation, $5*10^4$ cells were seeded in cell culture dish, after 24 h culturing in hypoxia condition, RBCp (250 μg/ml) was added into fresh medium and incubated for another 12 h. Then cells were treated with 808 nm NIR laser for various minutes (0 ~ 10 min), after incubation for another 30 min, then they were irradiated by 980 nm laser for 15 minutes. Finally, cells were stained by nonfluorescent dichlorofluorescein diacetate and DAPI for CLSM observation of ROS generation in cytoplasm.

4. Photoacoustic imaging *in vivo*

Animal model: All the animal procedures were in agreement with the guidelines of the Institutional Animal Care and Use Committee of Chinese Academy of Sciences and performed in accordance with the institutional guidelines on animal handling. HepG2 tumor was sheared into tissue blocks with size as 1mm*1mm*1mm and

resuspended in sterile PBS. These tissues were implanted subcutaneously into the right arm of 5 weeks old female nude mice.

***Photoacoustic imaging in vivo*:** The vascular blood O2 saturation was evaluated by multispectral photoacoustic imaging on the VisualSonics LAZR and Vevo 2100 Photoacoustic CT Scanner. After exposed with 808 nm NIR as a function of irradiation time from 0 to 10 min, oxygenated hemoglobin and total hemoglobin were measured at excitation wavelength of 850 and 750 nm after injected with pure RBC (200 μL) and RBCp (8 mg/mL, 200 μL).

Part B: Supplementary Figures

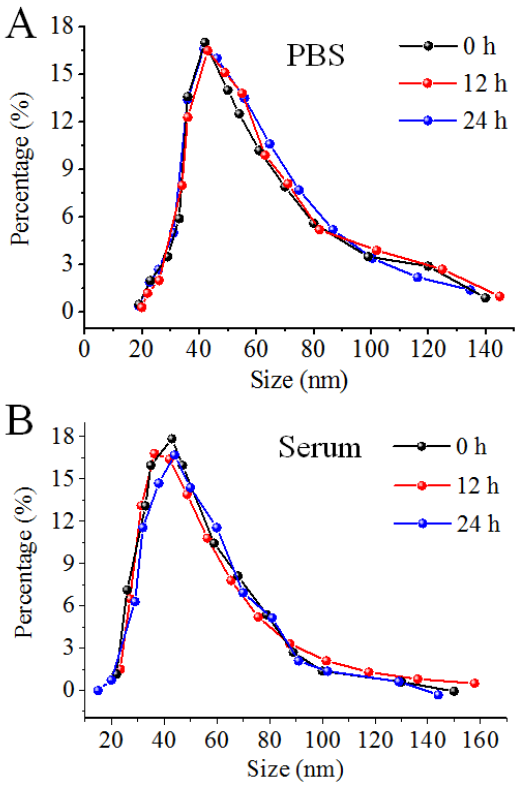

Figure S1. Dynamic laser scattering results of DSPE-PEG_{2000}-NH_2 modified UCNPs in PBS and Serum after incubating for different hours.

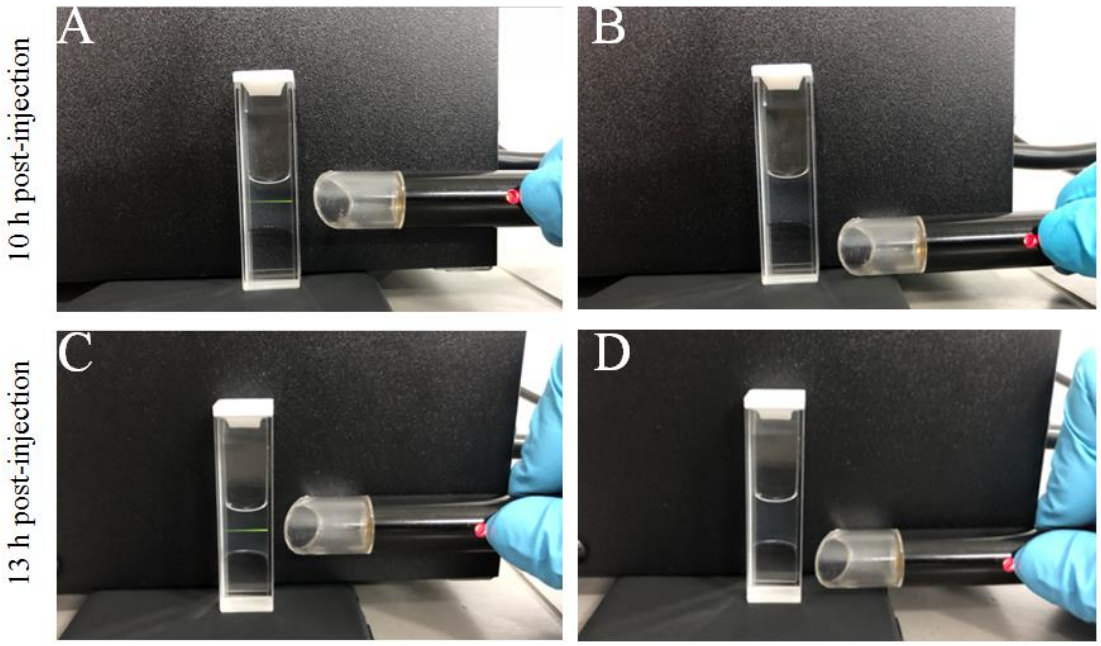

Figure S2. Photographs of the tumor homogenization solution (upper layer) and chloroform (lower layer) under 980 nm laser irradiation. The RBCp probes were intravenous injected, and the tumor tissues were harvested after 10 h and 13 h post-injection, then the tumor tissues were homogenized.

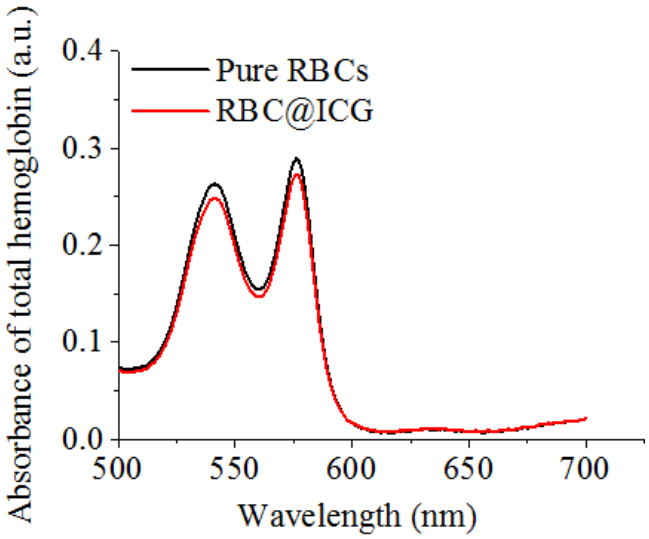

Figure S3. The total hemoglobin absorbance of pure RBCs and RBC@ICG.

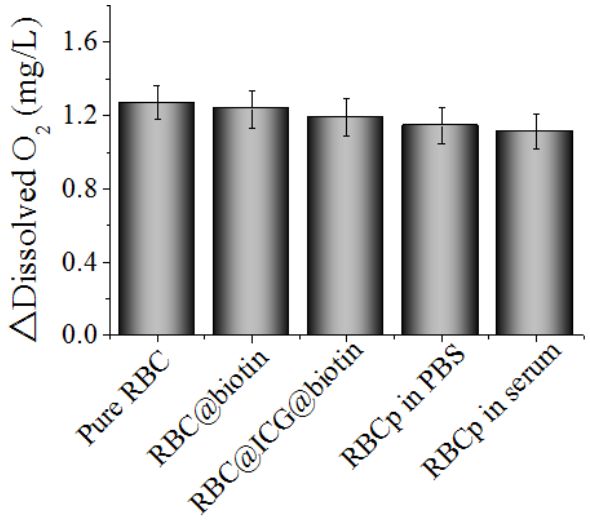

Figure S4. △Dissolved O_2 concentration of RBCs after stepwise functionalization. The data represents mean ± s.d. (n = 4).

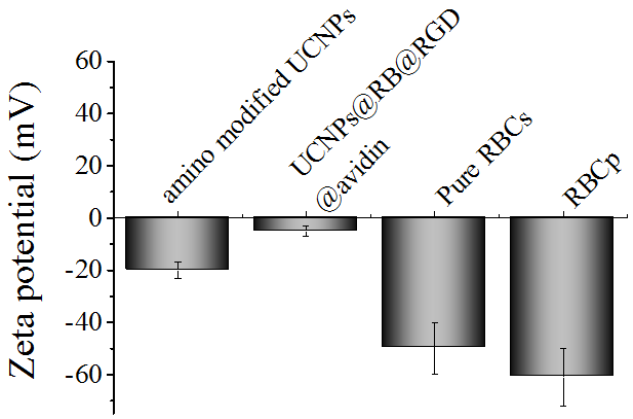

Figure S5. Zeta potential of anime modified UCNPs, UCNPs@RB@RGD@avidin, pure RBCs and RBCp. The data represents mean ± s.d. (n = 4).

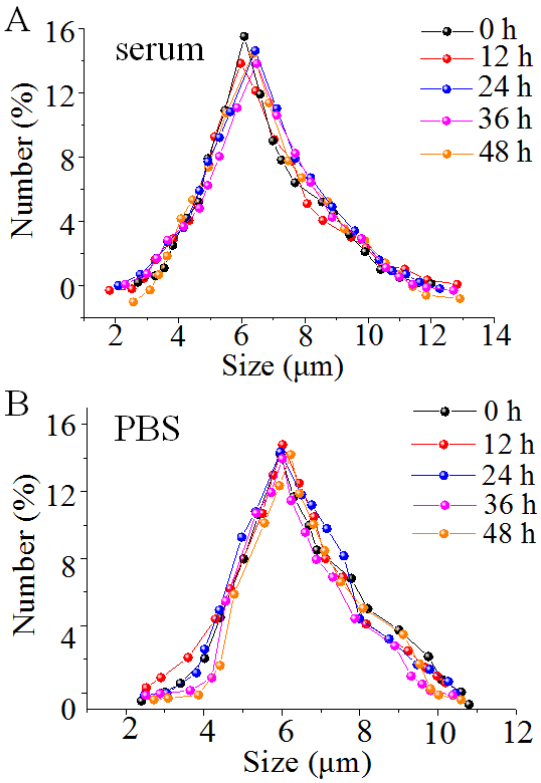

Figure S6. Size distribution of RBCp in serum (**A**) and PBS conditions at 37 °C for various time.

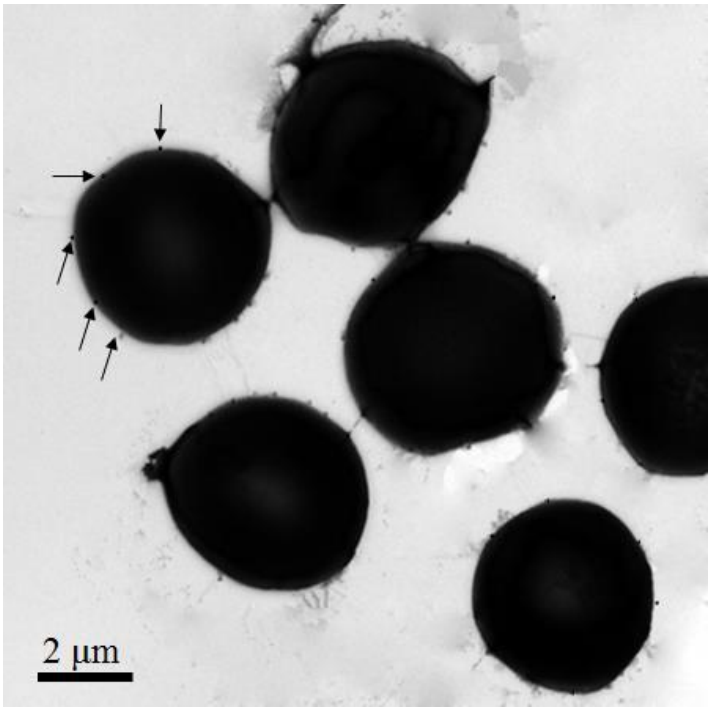

Figure S7. TEM image of RBCp. UCNPs can be observed on the membrane of RBCp (black arrows).

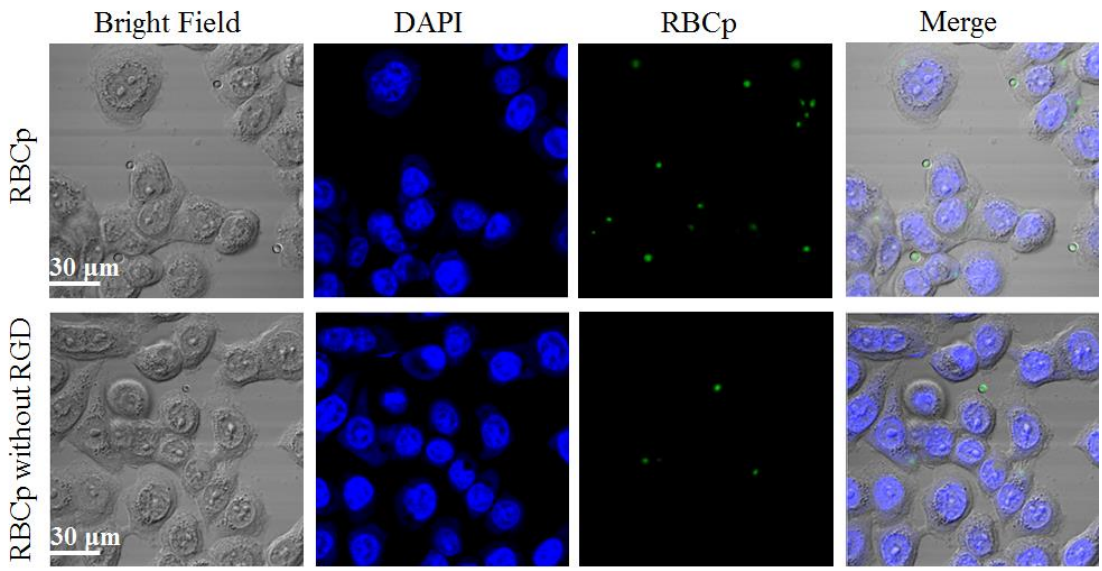

Figure S8. CLSM images of HepG2 cells after incubation with RBCp for 4 h. RBCp without RGD modification was used as control. Scale bar, 30 μm.

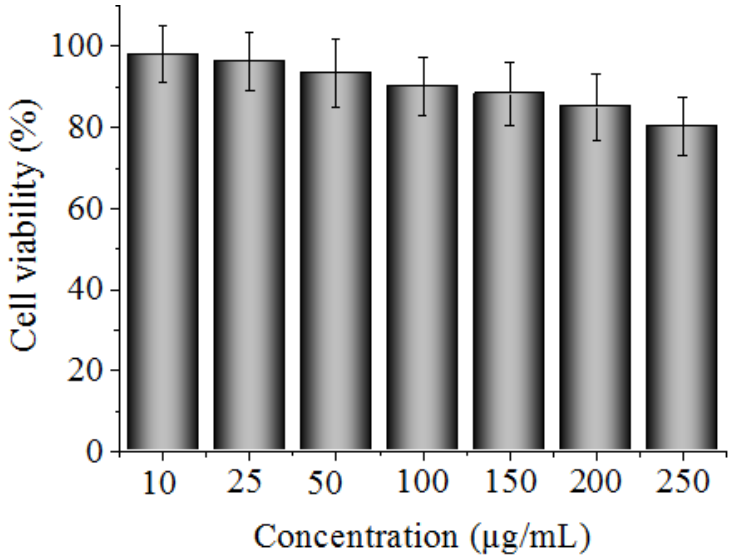

Figure S9. HepG2 cell viability after incubating with different concentration of RBCp for 24 hours. The data represents mean ± s.d. (n = 4).

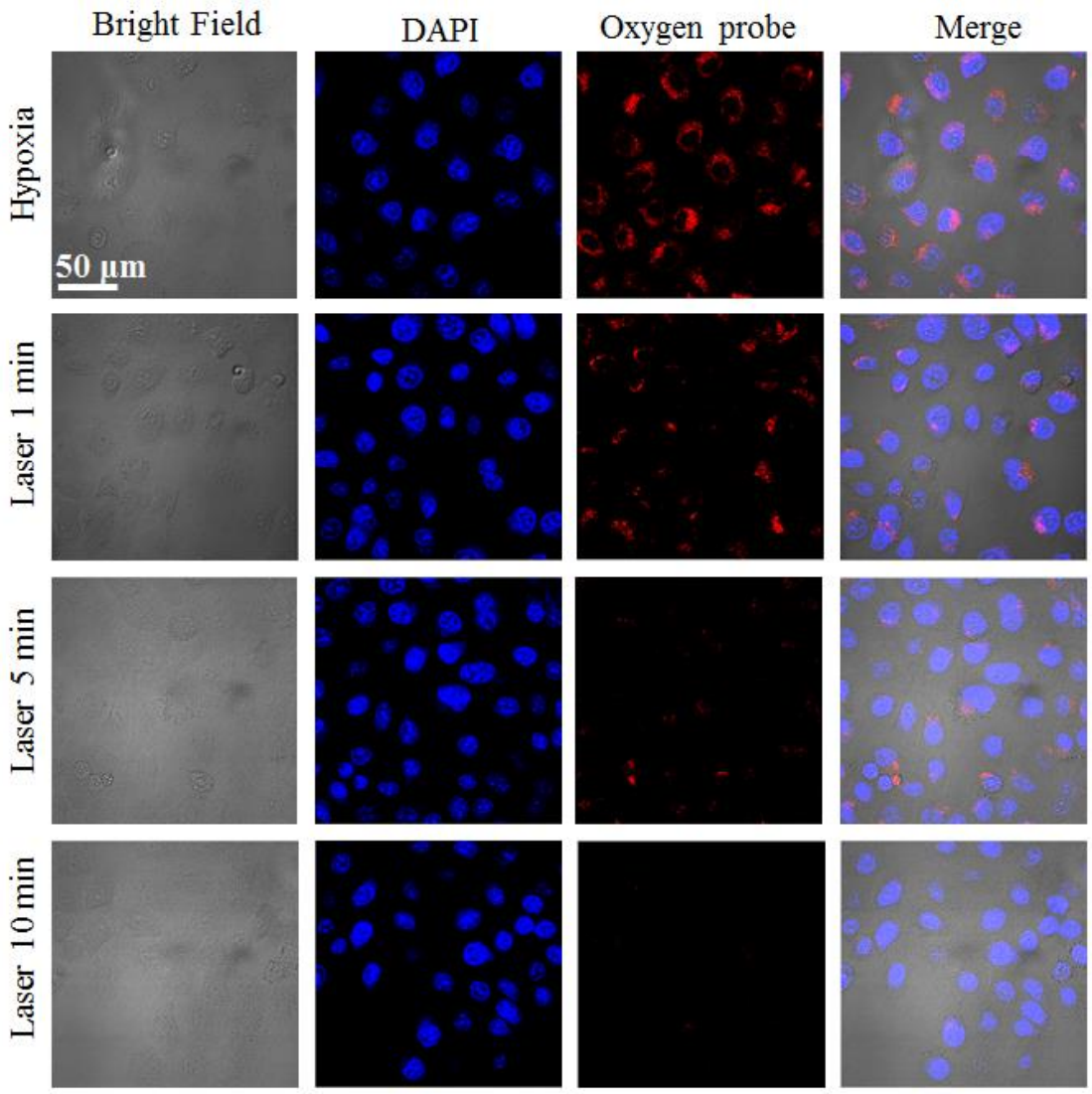

Figure S10. O_2 release in hypoxic HepG2 cells after incubation with RBCp for 4 h. Tris(4,7-diphenyl-1,10-phenanthroline) ruthenium(II) dichloride ($Ru(dpp)_3^{2+}$) was the oxygen indicator which can be quenched by O_2. CLSM images were obtained after exposure to 808 nm NIR laser for varied irradiation durations.

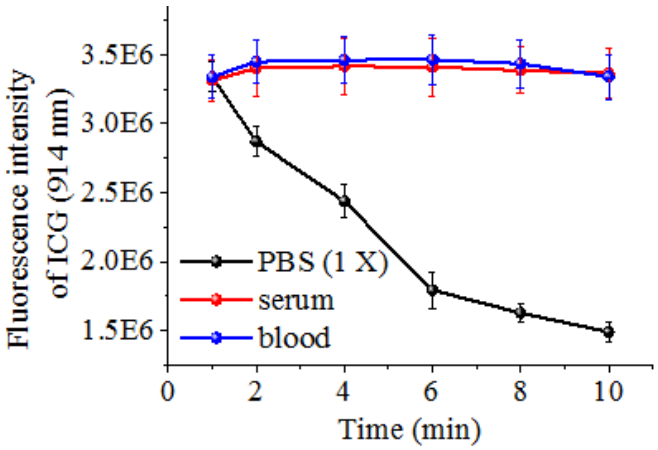

Figure S11. Photostability of ICG in a variety of biological media at 37 °C under 808 nm laser exposure at a power density of 0.5 W/cm^2 for 10 min. The data represents mean ± s.d. (n = 4).

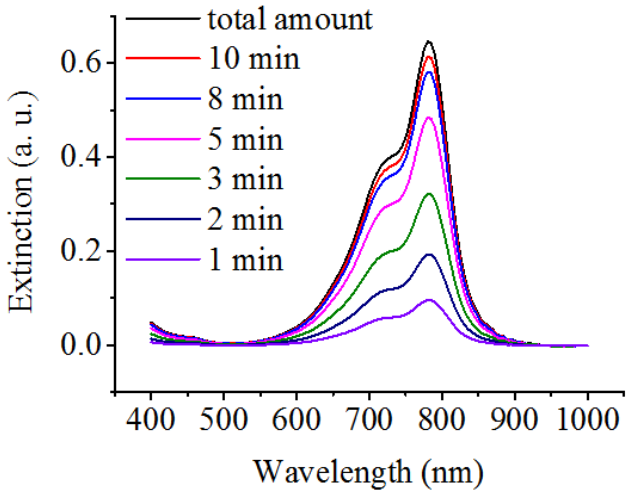

Figure S12. Extinction spectra of ICG in PBS after exposure to 808nm laser for various minutes.

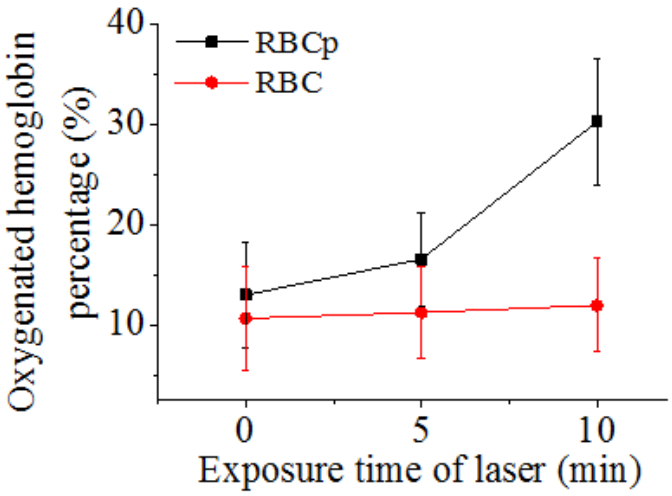

Figure S13. Oxygenated hemoglobin percentage of RBC and RBCp after exposure to 808 nm laser for varied irradiation durations. The data represents mean ± s.d. (n = 4).

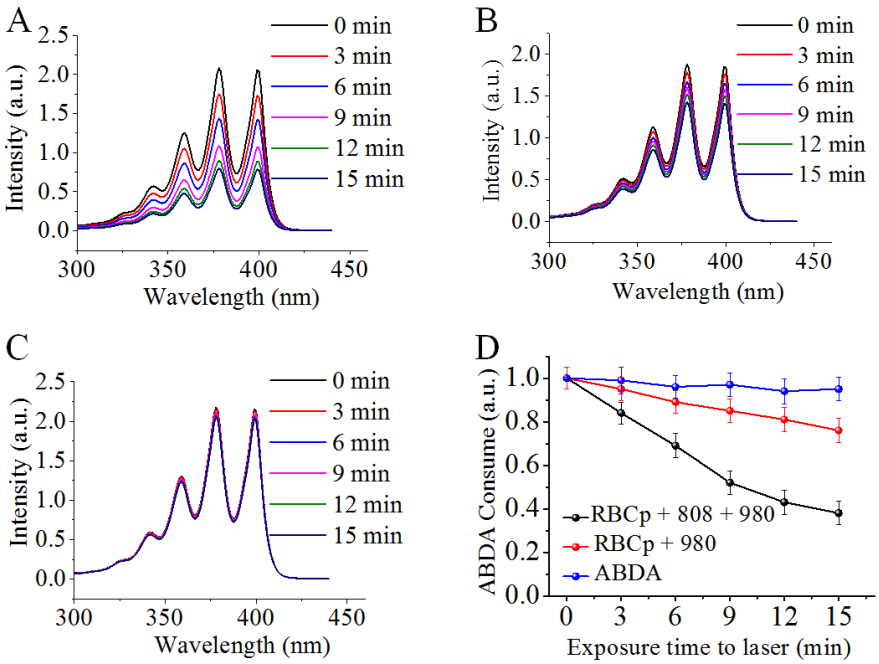

Figure S14. ABDA was incubated with RBCp, then with (A) or without (B) 808 nm laser irradiation for various times, afterwards they were both irradiated by 980 nm laser for 15 min, and the absorption spectra of ABDA were recorded. (C) The pure ABDA was firstly irradiated by 808 nm laser for various times, then exposed to 980 nm laser irradiation for 15 min, and the absorption spectra of ABDA were recorded as control. (D) Normalized absorbance changes of ABDA at 400 nm, indicating the $^{1}O2$ generation abilities under various conditions (A-C). The data represents mean ±

s.d. (n = 4).

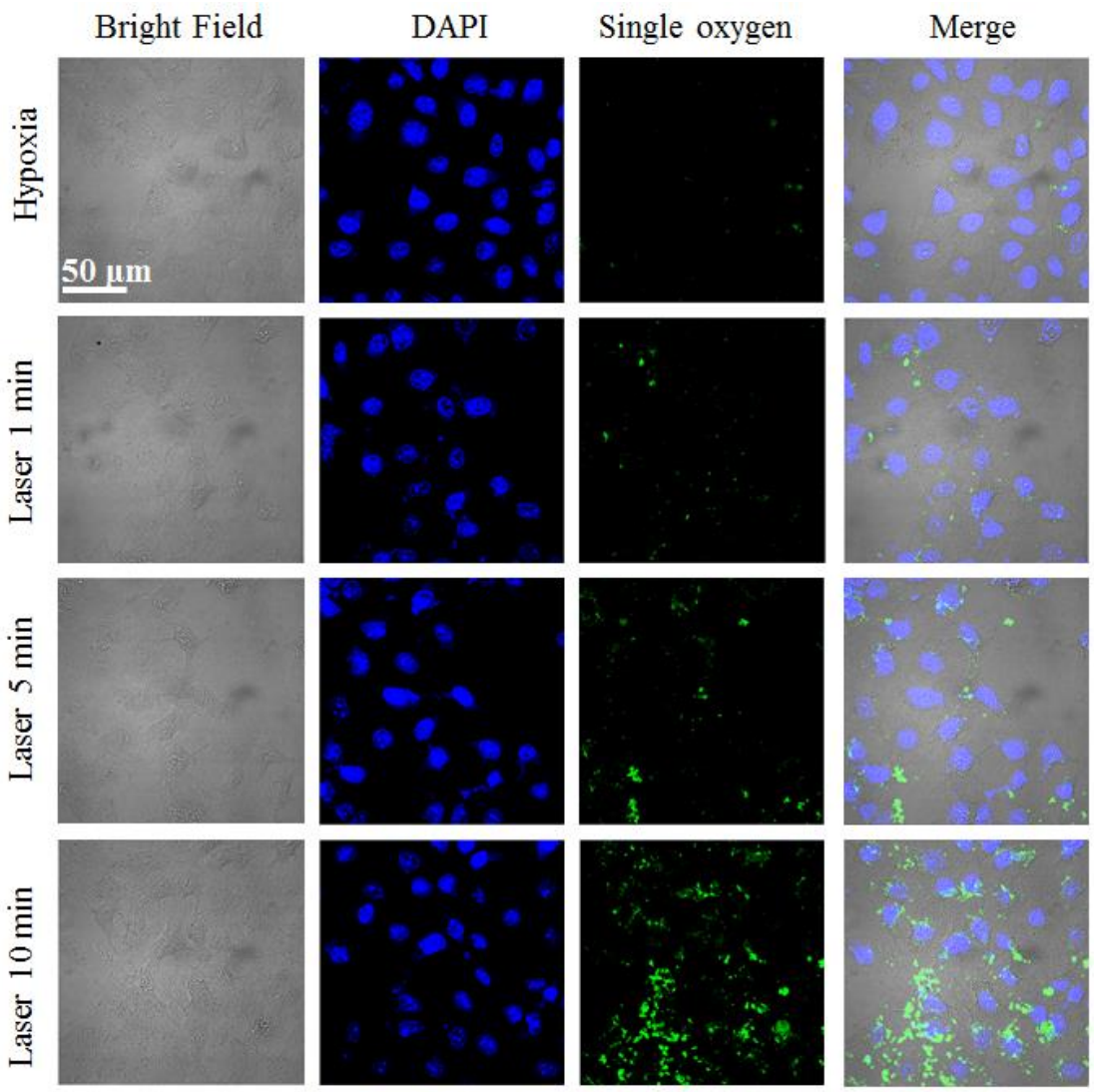

Figure S15. CLSM of ^{1}O generation in hypoxic HepG2 cells. With the extending of 808 nm laser exposure duration for O_2 release, stronger green fluorescence signals were increased after alternative 808 nm laser irradiation for 0 ~ 10 minutes and then 980 nm laser for 15 min.

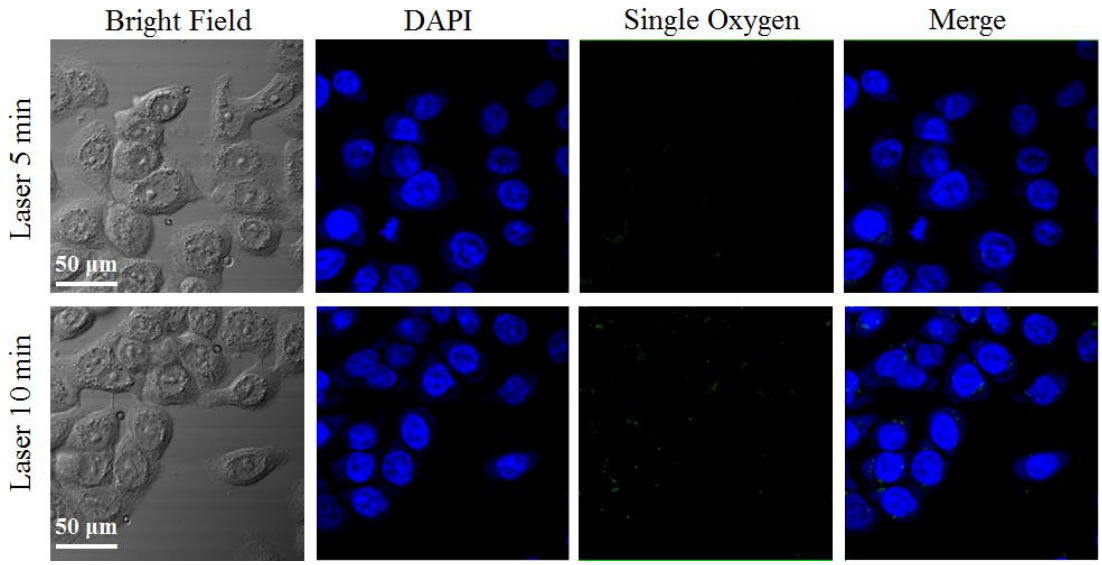

Figure S16. ^{1}O generation of RBCp in hypoxic HepG2 cells under 808 nm laser irradiation (0.5 W cm^{-2}, 5 min and 10 min).

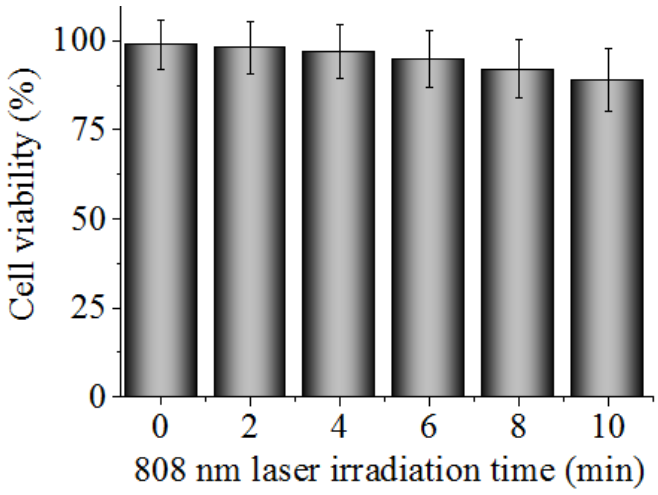

Figure S17. Cell viabilities of hypoxic HepG2 cells incubated with RBCp then under 808 nm laser irradiation (0.5 W cm^{-2} for different minutes). The data represents mean ± s.d. (n = 4).

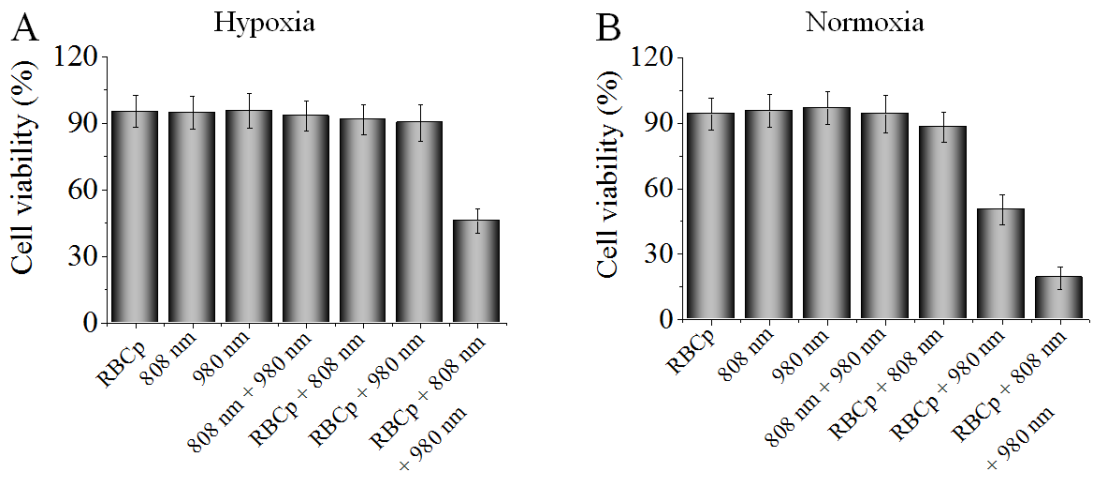

Figure S18. Cell viability of hypoxic (**A**) and normoxic (**B**) HepG2 cells with RBCp incubation then followed by alternately irradiating with 808nm and 980nm laser. The data represents mean ± s.d. (n = 4).

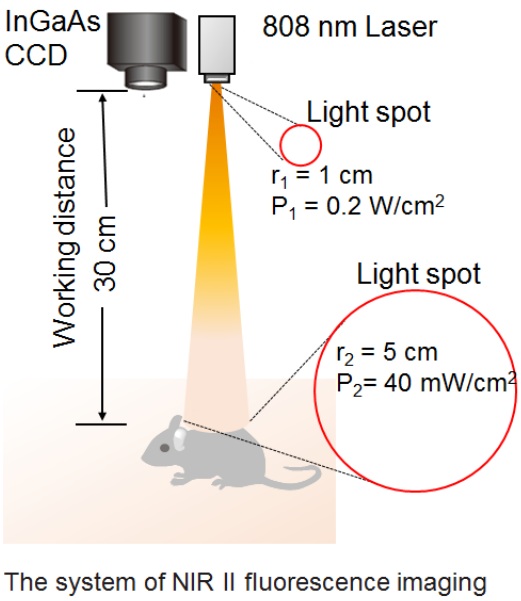

Figure S19. Schematic illustration of the NIR-II fluorescence imaging system for tumor surgical guidance. 30 cm working distance and 40 mW cm^{-2} fluence rate are used for the intraoperative imaging.

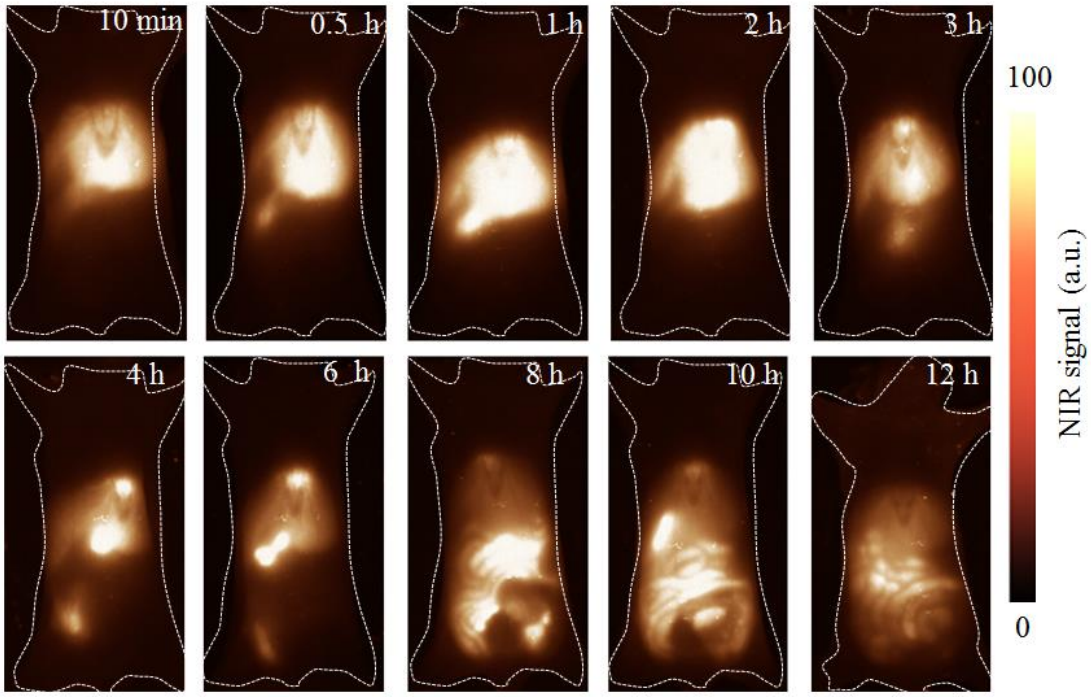

Figure S20. NIR-II fluorescence bioimaging results of subcutaneous tumor bearing mice after tail vein injection of ICG probes for various hours. ICG was severely accumulated in organs of the reticuloendothelial system and intensities, resulting in high background signals. Representative images are from n = 4.

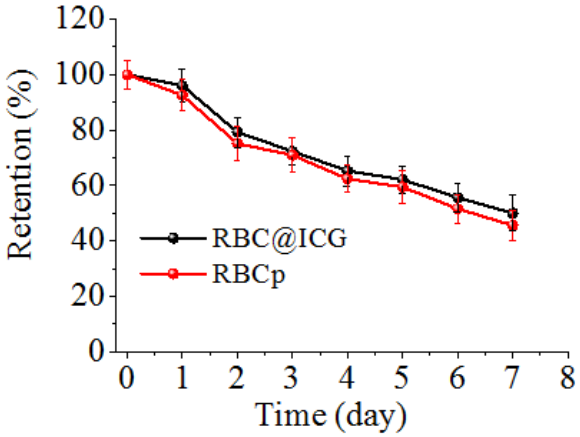

Figure S21. Blood retention of RBCp and RBC@ICG at different days after the tail vein injection. The data represents mean ± s.d. (n = 4).

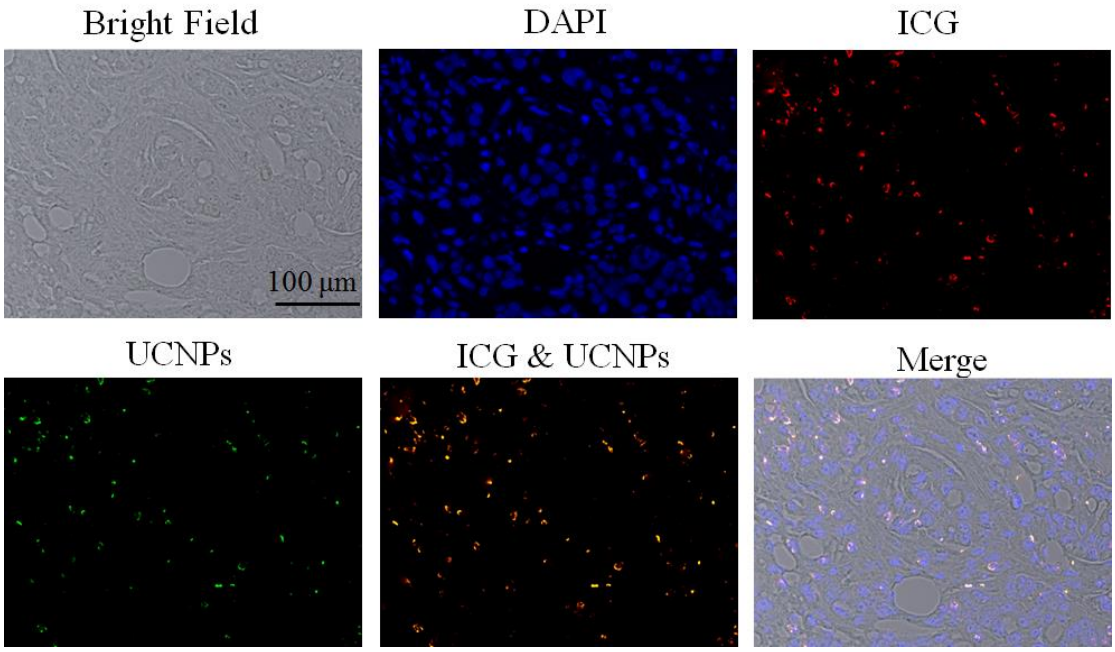

Figure S22. Fluorescence images of frozen tumor section (40 X) after 10 hours of RBCp intravenous injection. Red fluorescence (ICG) and green fluorescence (UCNPs) were successfully overlapped. Representative images were from n = 5.

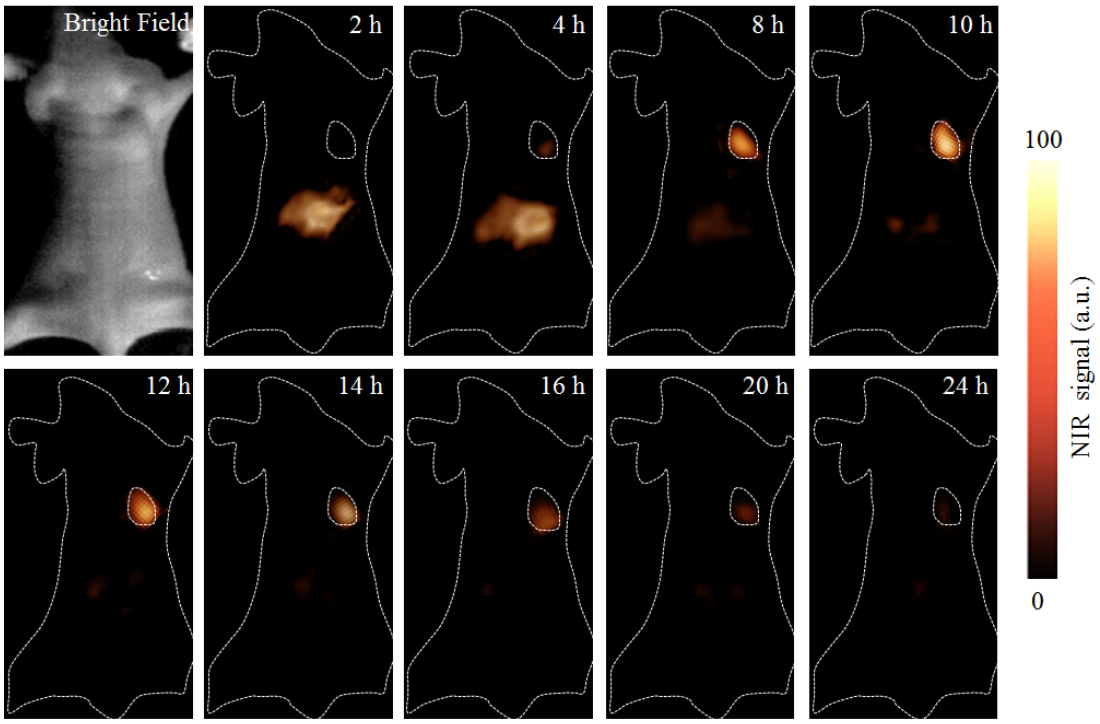

Figure S23. NIR-II fluorescence bioimaging for HepG2 epidermal ovarian tumor model (21 days after HepG2 cell subcutaneous injection) after tail vein injection of RBC@ICG@RGD. Representative images are from n = 4.

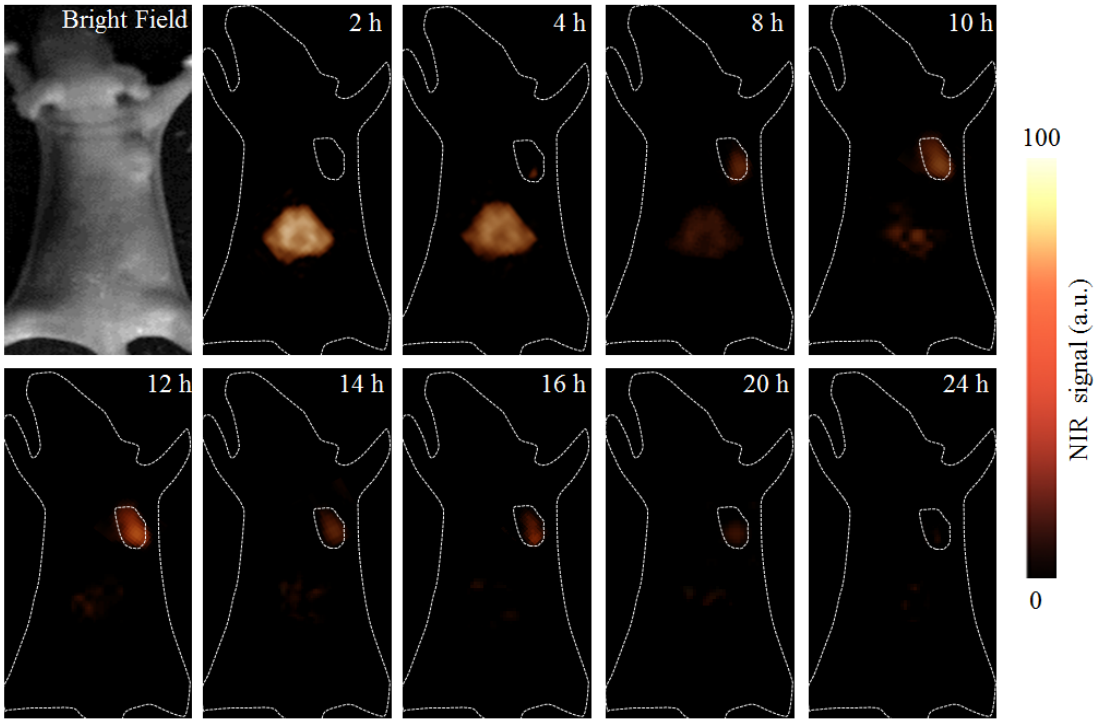

Figure S24. NIR-II fluorescence bioimaging for HepG2 epidermal ovarian tumor model (21 days after HepG2 cell subcutaneous injection) after tail vein injection of RBCp without RGD modification. Representative images are from n = 4.

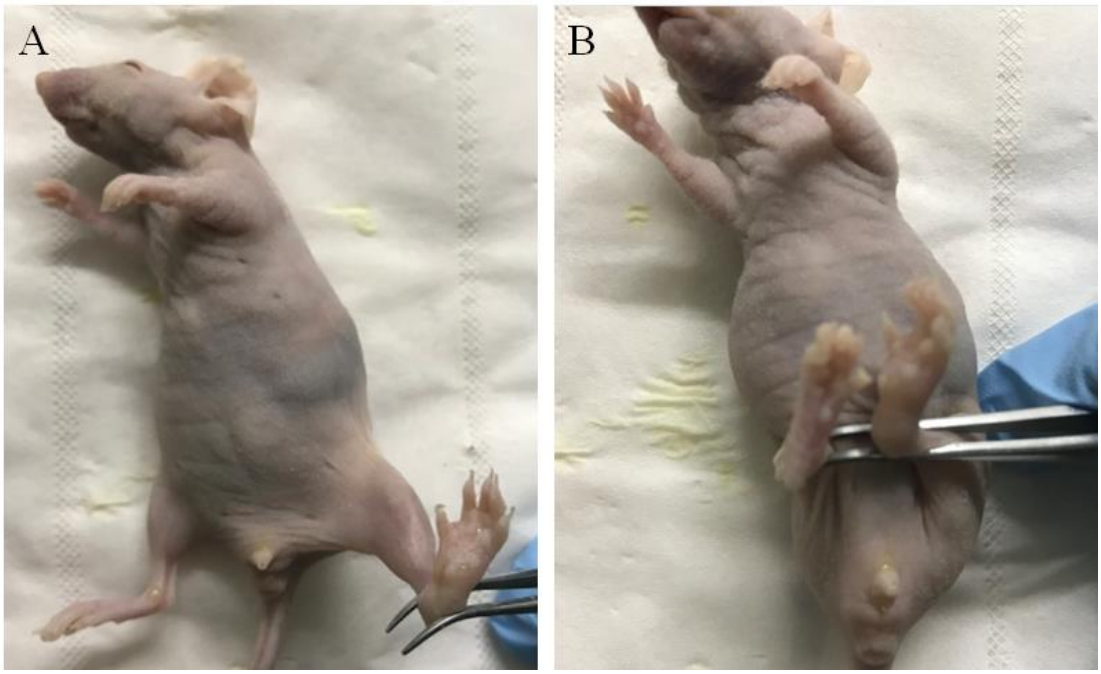

Figure S25. A popliteal lymph node metastasis model by intradermal injected HepG2 cells (5 *10^8 cells/mouse) to the hind paw of five-week-old mice for 3 weeks. Digital images of mice with normal right legs and left legs with intradermal hind paw injection of HepG2 cells after 10 days (**A**) and 21 days (**B**).

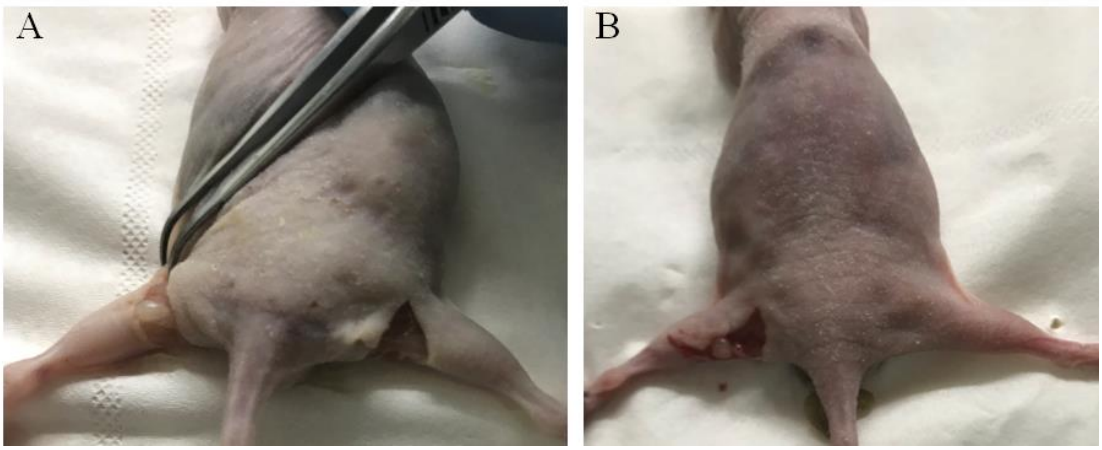

Figure S26. Digital images of mice with a popliteal lymph node metastasis in the left leg and normal right leg (**A**). Digital image of another popliteal lymph node metastasis-bearing mice (**B**).

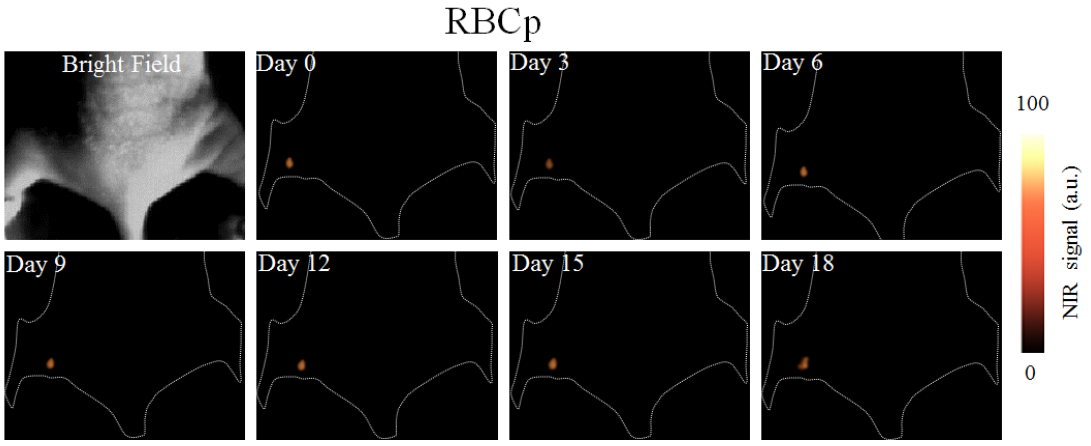

Figure S27. NIR-II fluorescence bioimaging of popliteal lymph node metastasis-bearing mice for different days after intravenous injection of RBCp (the RBCp was injected 10 hours before each imaging). Representative images are from n = 4.

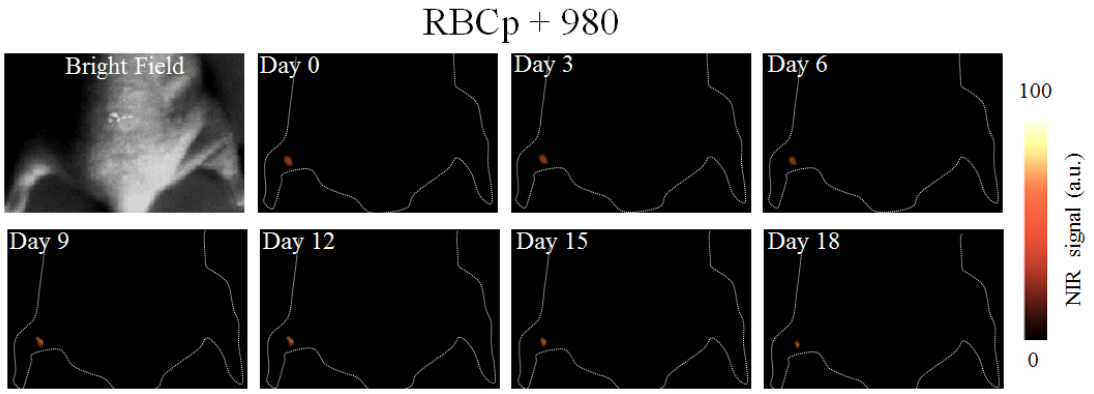

Figure S28. NIR-II fluorescence bioimaging-guided PDT for popliteal lymph node metastasis-bearing mice. The RBCp was injected 10 hours before each treatment and imaging, then the mice were irradiated with 980 nm laser for 10min after 10 hours of injection. Representative images are from n = 4.

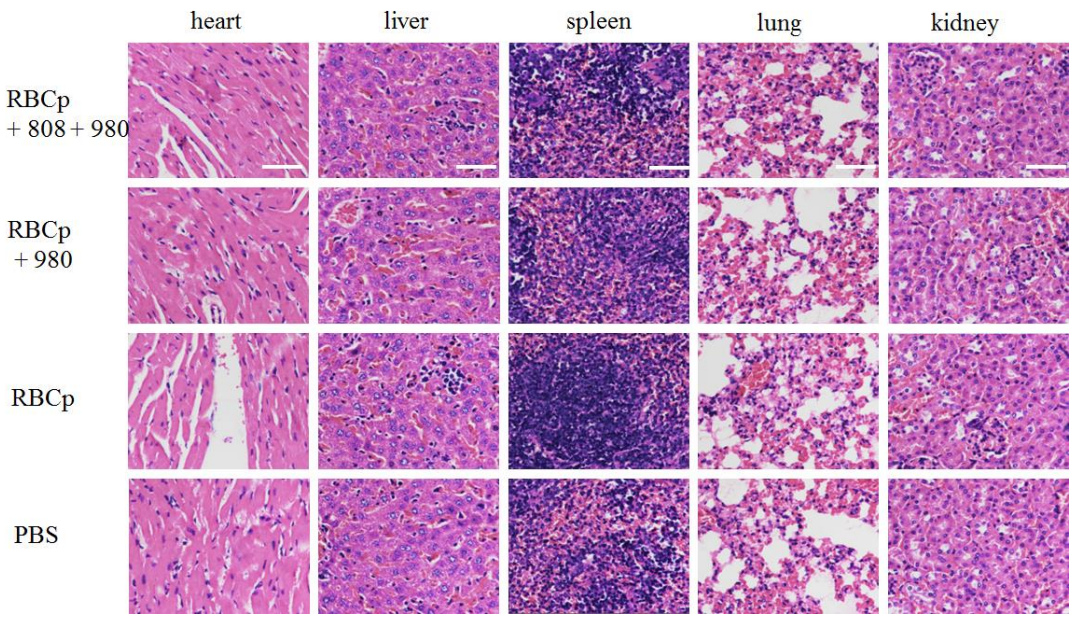

Figure S29. H&E-stained slices of major organs, from top to bottom: RBCp + 808-nm + 980-nm laser; RBCp + 980-nm laser; RBCp; PBS. Scale bars, 100 μm. Representative images are from n = 4.

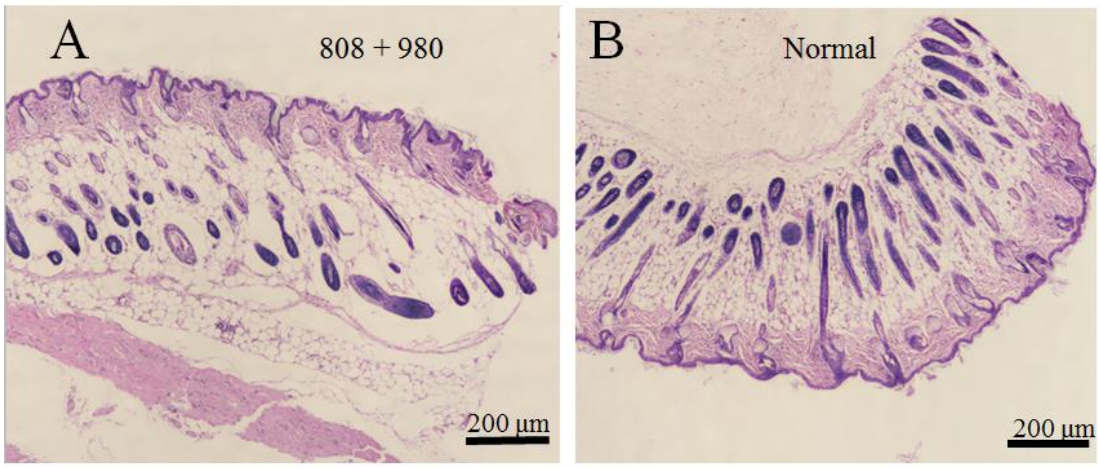

Figure S30. (**A**) H & E staining of mouse skin after being irradiated by 808 nm and 980 nm laser (808nm laser = 0.5 W cm^{-2}, time = 10 min; 980nm laser = 1.5 W cm^{-2}, time = 15 min; 5 min laser exposure with 5 min intervals). (**B**) H & E staining of mouse skin without laser irradiation. Representative images are from n = 4.

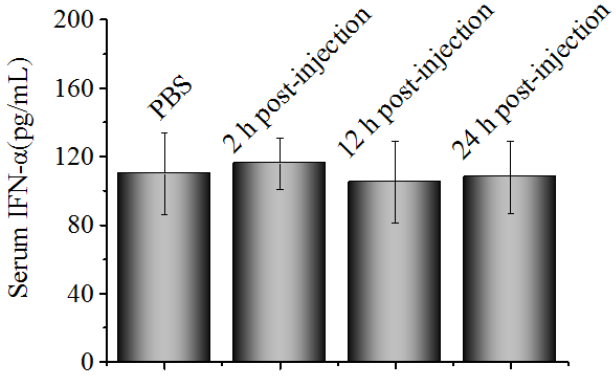

Figure S31. Serum immune response analysis of RBCp injection after 2, 12, 24 hours, with PBS injection as control. Serum IFN-α release was not detected after injection of RBCp, indicating immune responses could be excluded for the *in vivo* bioimaging. Mean ± s.d. from n = 4.